

Relay Element Performance During Power System Frequency Excursions

Daqing Hou

Schweitzer Engineering Laboratories, Inc.

Presented at the
61st Annual Conference for Protective Relay Engineers
College Station, Texas
April 1–3, 2008

Originally presented at the
34th Annual Western Protective Relay Conference, October 2007

Relay Element Performance During Power System Frequency Excursions

Daqing Hou, *Schweitzer Engineering Laboratories, Inc.*

Abstract—Many voltage and current protection elements in microprocessor relays use the fundamental frequency component of current and voltage. Distance relays also calculate apparent fault impedance at the power system frequency. Most microprocessor relays track system frequency to calculate the current, voltage, and impedance quantities. When the integrity of the power system is in jeopardy, system frequency can experience a large and rapid excursion because of generation and load imbalances from system separations into regional islands. Such separations occur in major system events such as the U.S.-Canadian blackout of August 14, 2003, that affected 50 million people in eight U.S. states and two Canadian provinces. Relay elements in such a disturbed system state must perform reliably to prevent any protective element misoperations from aggravating the disturbance and causing widespread outages. Relay element performance during a system frequency excursion depends on factors including the system frequency rate of change, the tracking rate and tracking limit of the relay, and the element type. This paper reviews overcurrent, distance, and current differential element designs. It then examines the performance of these elements during frequency excursions.

I. INTRODUCTION

Microprocessor relays use numerical algorithms to calculate phasors from voltage and current inputs based on either the power system nominal frequency or the actual measured frequency. Relays use voltage and current phasors to construct different protection elements such as overcurrent, current differential, and distance elements. Different filters help relays reduce the impact of noises on phasor calculation and improve overall protection element accuracy.

The power system frequency, although generally stable, seldom remains at the nominal value. Major system disturbances such as load shedding or generation shutdowns can cause great imbalance between load and generation, and the system frequency can experience a sudden significant change. Protective relays should be stable during a system frequency excursion to prevent misoperations that can further degrade system stability.

Different protection elements behave differently for the same frequency excursion. Different relay designs also significantly impact the behavior of protection elements. Protection engineers must understand and predict protection element performance during adverse system conditions to operate and control the system better.

Many relay design aspects influence protection element performance during a system frequency excursion. These include the following:

- the type of filtering a relay employs to process the input signal and construct the phasor

- whether the relay has a frequency tracking algorithm that adapts sampling frequency to the system frequency
- the method by which a relay measures system frequency
- frequency tracking limits and tracking speed (time constant)
- the type of polarizing memory that the impedance element uses

In this paper, we first review some major filtering and phasor calculation algorithms and evaluate the impact of a frequency excursion on these filters. We then examine frequency tracking and some design parameters such as frequency tracking limits and tracking speed. Finally, we examine in detail three major protection elements to reveal how these elements perform during system frequency changes.

II. REVIEW OF PHASOR ESTIMATION ALGORITHMS

We normally use a phasor to represent a sinusoidal quantity with a constant frequency. With fixed frequency, two numbers are sufficient to define the phasor quantity: magnitude and angle. Equation (2) defines the phasor for the sinusoidal quantity of (1):

$$i(t) = I_m \cos(\omega t + \theta) \quad (1)$$

$$I = \frac{I_m}{\sqrt{2}} e^{j\theta} = \frac{I_m}{\sqrt{2}} (\cos\theta + j\sin\theta) \quad (2)$$

When an input is a pure sinusoidal quantity, we can use any two input samples to calculate the phasor. Suppose ΔT is the sampling interval:

$$i_k = I_m \cos(\omega k \Delta T + \theta) \quad (3)$$

$$\begin{aligned} i_{k-1} &= I_m \cos[\omega(k-1)\Delta T + \theta] \\ &= I_m \cos(\omega k \Delta T + \theta) \cos(\omega \Delta T) + I_m \sin(\omega k \Delta T + \theta) \sin(\omega \Delta T) \\ &= i_k \cos(\omega \Delta T) + I_m \sin(\omega k \Delta T + \theta) \sin(\omega \Delta T) \end{aligned} \quad (4)$$

From (4), we have

$$I_m \sin(\omega k \Delta T + \theta) = \frac{1}{\sin(\omega \Delta T)} i_{k-1} - \frac{\cos(\omega \Delta T)}{\sin(\omega \Delta T)} i_k \quad (5)$$

Recognize that $I_m \sin(\omega k \Delta T + \theta)$ is the quadrature part of the phasor we seek; two input samples then express the phasor:

$$I_k = \frac{1}{\sqrt{2}} \left[i_k + j \frac{i_{k-1} - i_k \cos(\omega\Delta T)}{\sin(\omega\Delta T)} \right] \quad (6)$$

Equation (6) defines a rotating phasor for which the angle advances $\omega\Delta T$ radians each time a new sample is available for phasor calculation. This time-varying nature of the phasor is of no significance for protection algorithms that use magnitudes and phasor ratios such as overcurrent and impedance elements.

The quadrature part of the phasor in (6) comes from a high-pass filtering process with the frequency magnitude response in Fig. 1 for a sampling frequency of 16 samples per cycle. A faster sampling rate magnifies more high frequency contents of the signal.

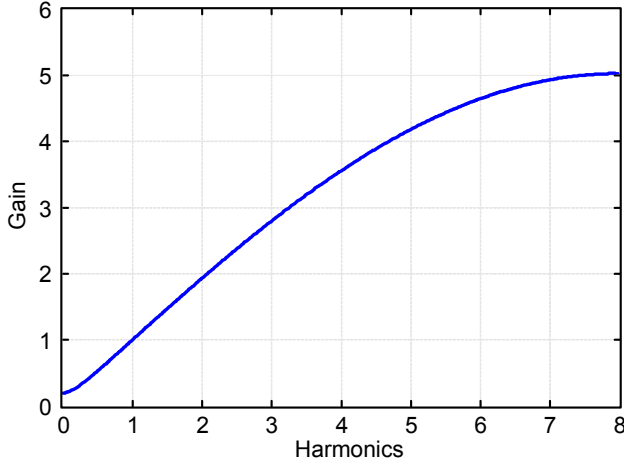


Fig. 1. Frequency Response of Phasor Calculation Using Two Samples.

Current and voltage measurements used in protective relays contain many unwanted components that, without proper filtering, degrade the accuracy of the relaying elements. These unwanted components include the exponentially decaying dc offsets of currents, capacitor-coupled voltage transformer (CCVT) transients of voltages, sub-frequency resonances from series-capacitor compensated systems, harmonics from CT saturations, transformer inrushes, and power electronics. Reference [1] evaluated many digital filter algorithms and proposed a total filtering concept. Most microprocessor relays today use either the one-cycle cosine filter of (7) or the one-

$$i_{out,k} = \frac{2}{N} \sum_{n=1}^N i_{m,k-N+n} \cos \left(\frac{2\pi(n-0.5)}{N} \right) \quad (7)$$

$$I_{out,k} = \frac{\sqrt{2}}{N} \sum_{n=1}^N i_{m,k-N+n} \cdot e^{-j\frac{2\pi n}{N}} = \frac{\sqrt{2}}{N} \left\{ \sum_{n=1}^N i_{m,k-N+n} \cos \left(\frac{2\pi n}{N} \right) - j \sum_{n=1}^N i_{m,k-N+n} \sin \left(\frac{2\pi n}{N} \right) \right\} \quad (8)$$

cycle Fourier filter of (8) to eliminate or reduce the impact of undesired components on the phasor calculation. Variations of these filters improve filtering speed and accuracy. The capability of filtering out unwanted input components remains essentially the same. Let N be the number of samples per cycle, as in (8).

The cosine filter output is an instantaneous sinusoidal quantity. From this output, either (6) or a quarter-cycle delay [1] produces the phasor we want. The cosine filter in (7) has a double differentiator property that eliminates both dc and ramp components of an input. The filter, therefore, is effective rejecting the exponentially decaying dc component.

The Fourier filter output directly provides a phasor quantity, but it doubles the calculation. The sine portion of the Fourier filter does not reject the ramp component of an input, so additional differentiation is necessary to effectively reject the exponentially decaying dc. We can use either hardware or firmware to implement this additional differentiation. A simple digital differentiator such as $[i_k - i_{k-1}]$ is as effective as a mimic filter that matches the system X/R ratio.

Phasors from the cosine and Fourier filters are rotating phasors such as that in (6). We can use the recursive form of the Fourier filter [2] to derive a stationary phasor:

$$I_k = I_{k-1} + \frac{\sqrt{2}}{N} (i_k - i_{k-N}) e^{-j\frac{2\pi}{N}} \quad (9)$$

The recursive form of the Fourier filter is computationally efficient. For each new input sample, the filter derives a new phasor from a difference of input samples one cycle apart, an angle adjustment of the difference between these samples, and a single addition operation. Despite the efficiency of the filter, application of it in modern microprocessor relays is uncommon. One reason is that the filter has an infinite-impulse response property. If a bad input sample gets through a relay data acquisition system, the impact on the phasor output can last a significantly long time.

However, the recursive Fourier filter is a good starting point for analyzing filter behavior when the sinusoidal input to the filter has an off-nominal frequency. Assume that the input frequency is $\Delta\omega$ radians per second apart from the normalized frequency 2π , as in (10).

$$\begin{aligned}
i_k - i_{k-N} &= I_m \left[\cos \left(\frac{k(2\pi + \Delta\omega)}{N} + \theta \right) - \cos \left(\frac{(k-N)(2\pi + \Delta\omega)}{N} + \theta \right) \right] \\
&= I_m \left[\cos \left(\frac{k(2\pi + \Delta\omega)}{N} + \theta \right) - \cos \left(\frac{k(2\pi + \Delta\omega)}{N} - \Delta\omega + \theta \right) \right] \\
&= -2I_m \sin \left(\frac{k(2\pi + \Delta\omega)}{N} - \frac{\Delta\omega}{2} + \theta \right) \sin \left(\frac{\Delta\omega}{2} \right)
\end{aligned} \tag{10}$$

Combination of (9) and (10) yields a stationary phasor that we can express as a function of frequency deviation $\Delta\omega$ from the nominal:

$$\begin{aligned}
I_k &= I_{k-1} - \frac{2\sqrt{2}}{N} I_m \sin \left(\frac{\Delta\omega}{2} \right) \cdot \\
&\quad \sin \left(\frac{k(2\pi + \Delta\omega)}{N} - \frac{\Delta\omega}{2} + \theta \right) e^{-j\frac{2\pi}{N}}
\end{aligned} \tag{11}$$

Equation (11) shows that when the input frequency differs from the frequency the filtering system assumes, output phasor modulation occurs. The amount of modulation is a sinusoidal quantity with a magnitude proportional to $\sin(\Delta\omega/2)$ and a period of $2\pi + \Delta\omega$. Fig. 2 shows a phasor variation when the input frequency is 5 Hz less than the nominal 60 Hz, or a $\Delta\omega$ of -0.5236 radians per second. We assume that the initial phasor is at $1\angle 0^\circ$. Fig. 3 shows the phasor magnitude plot for the same input with a one per-unit magnitude.

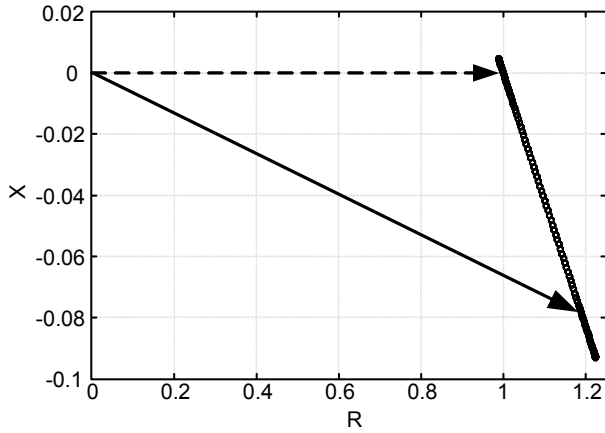


Fig. 2. Phasor Oscillation for a 55 Hz Input

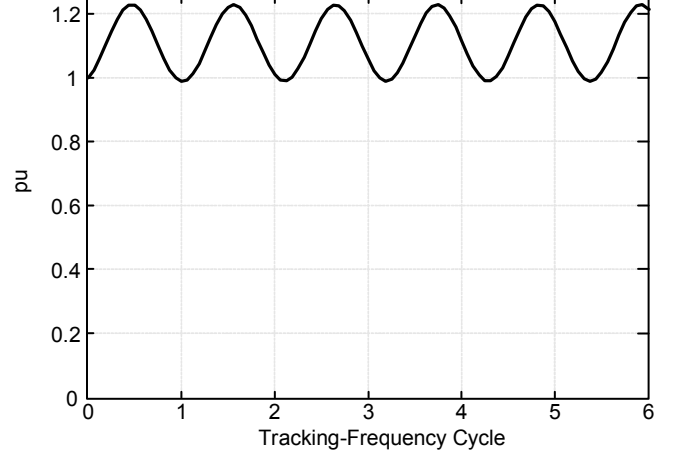


Fig. 3. Magnitude Oscillation of Static Recursive Phasor, for a 55 Hz Input.

Derivation of a closed-form expression of cosine and Fourier filter magnitudes for off-nominal frequency inputs involves significant calculation. These magnitudes depend on individual phasor algorithm and differ for cosine with a quarter-cycle delay, cosine with a two-sample phasor calculation, Fourier, and Fourier plus a differentiator. For all algorithms, oscillation magnitude is proportional to the $\sin(\Delta\omega/2)$ factor. In addition, the oscillation frequency doubles to $2(2\pi + \Delta\omega)$ because magnitude calculation includes taking the square root of the sum of squares.

Fig. 4 shows the phasor magnitude oscillations of three phasor calculation algorithms: cosine filter plus a quarter-cycle delay, Fourier filter, and Fourier plus a differentiator $[i_k - i_{k-1}]$. The input has a frequency of 55 Hz and one per-unit magnitude.

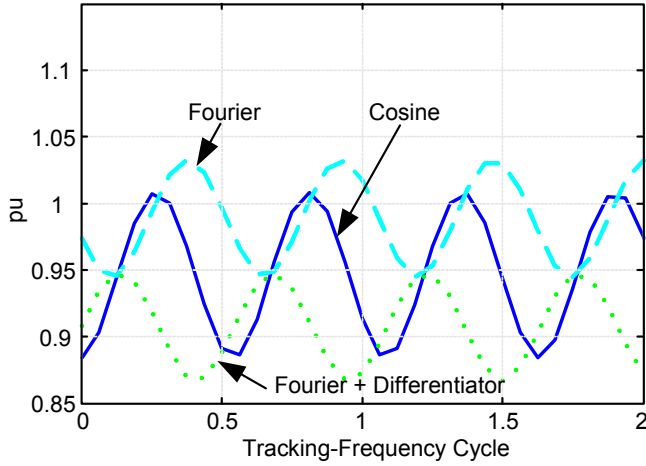


Fig. 4. Magnitude Oscillation of Cosine, Fourier, and Fourier Plus Adjacent-Sample Differentiator Filters, for a 55 Hz Input

For comparison, Fig. 5 shows the magnitude oscillation for a 65 Hz input.

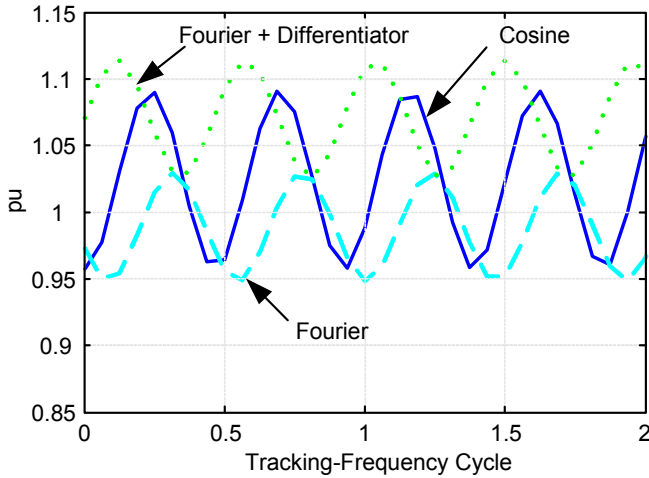


Fig. 5. Magnitude Oscillation of Cosine, Fourier, and Fourier Plus Adjacent-Sample Differentiator Filters, for a 65 Hz Input.

III. SAMPLING FREQUENCY ADJUSTMENT

From the previous section, we see that a mismatch between the frequency the relay calculates and the input signal leads to calculated phasor errors in both magnitude and angle. In normal power system operations, system frequency is very close to nominal frequency. Assuming the frequency of relaying inputs to be at the nominal frequency generates little error. For example, if the input frequency is 59.8 Hz, the phasor magnitude error of assuming the nominal frequency is proportional to $\sin(\Delta\omega/2)$ or about one percent.

However, power systems can experience large frequency excursions during load shedding or generation rejections. Protective relays should remain secure during these critical system states. Many microprocessor relays employ frequency tracking algorithms to ensure that system frequency changes have minimal impacts on relay phasor measurement and protection elements. These relays monitor the system frequency continuously and adjust the signal sampling rate so as to maintain a constant number of samples per measured frequency cycle. Some literature refers to this frequency tracking as adaptive sampling. Common sampling rates are 4, 8, 12, 16, 24, or 32 samples per cycle.

A. Frequency Measurement

The first step of frequency tracking is to measure power system frequency. Different frequency measurement algorithms exist [2]. The most common frequency measurement method is to measure the time elapsed between the zero crossings of the input signals. The inverse of this time is twice the system frequency. The following input quantities are available for this purpose:

- Single-phase voltage
- A combination of three-phase voltages such as alpha component of voltages: $v_\alpha = v_a - [(v_b + v_c)/2]$
- Single-phase current
- Combination of all three-phase currents such as alpha component of currents: $i_\alpha = i_a - [(i_b + i_c)/2]$

Voltages are good choices for the zero-crossing measurement because they have high magnitudes and minimum harmonic contents. For current-only relays, we must use currents with proper filtering and smoothing for zero-crossing measurement. The advantage of using a combination of all three-phase quantities is that we can still obtain the measurement during loss of one or two phases, such as in a single-pole open condition. A zero crossing is only available every half cycle, so the frequency measurement using a single-phase input cannot be faster than a half cycle. Measuring zero-crossings on all three phases simultaneously accelerates the frequency measurement to as fast as every one-sixth of a cycle.

As in the phasor calculation, voltage and current components other than the sinusoidal quantity degrade zero-crossing measurement accuracy. These components include harmonics, white noise, and exponentially decaying dc, which has the greatest impact on the zero-crossing measurement. Pre-filtering with either or both low-pass or cosine filters before zero-crossing measurement can attenuate these components. The cosine filter reduces harmonics rather than rejecting them completely, because the cosine filter coefficients are not synchronized with the input frequency.

Post-filtering also improves frequency measurement. The most common type of filter is a simple low-pass averaging filter. We measure several zero-crossings and average them before calculating the frequency. One averager is the so-called Olympic filter. With several measurements, the Olympic filter rejects the largest and smallest measurements and then averages the remaining measurements.

While improving frequency measurement accuracy, the pre- and post-filtering processes add delay to the measurement. Too much delay can open a window within which the phasor calculation can be inaccurate enough to impact the protection elements. As with protective element filtering, there must be a balance between frequency measurement accuracy and speed.

Fig. 6 shows the speed comparison of several frequency measurements. The input frequency has a 2-Hz step change at cycle one. A step change in frequency is not a power system phenomenon because of inertia involved in a real system. We use a step change here only to illustrate the responses of different measurement algorithms. The frequency measurements in Fig. 6 all use positively going zero-crossing detection of a single-phase voltage, so a frequency measurement is available every one cycle. The voltage is purely sinusoidal. From Fig. 6, we see that the frequency measurement with 4-point post average smoothing provides a true frequency indication four cycles after the frequency step change. With additional one-cycle cosine pre-filtering, the true frequency measurement is delayed a further cycle. Further post-filtering with 8-point average smoothing delays the available true frequency measurement accordingly. Note that Fig. 6 does not show the benefits of pre- and post-filtering because the input includes no noise.

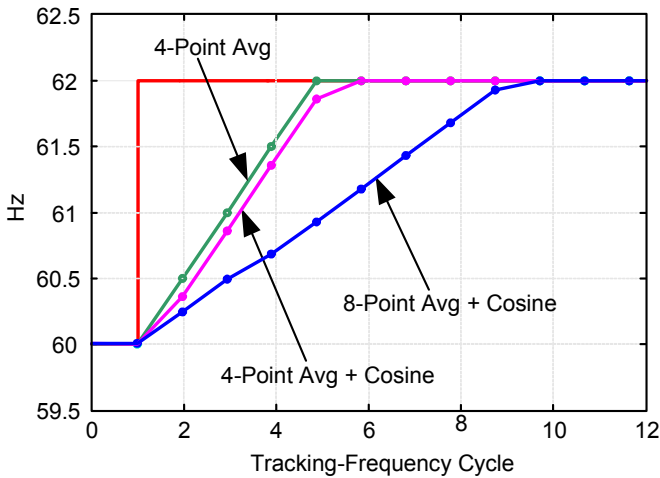


Fig. 6. Frequency Measurements With Different Pre- and Post-Filtering

Fig. 7 shows frequency measurements when the input signal contains five percent third harmonic and one percent white noise. We see that, without proper pre-filtering and sufficient post-filtering, the frequency measurement of the 4-point averager yields an error of about 60 mHz. The cosine filter dramatically reduced the effect of the third harmonic, and the longer smoothing reduces the effect of white noise on the measurement.

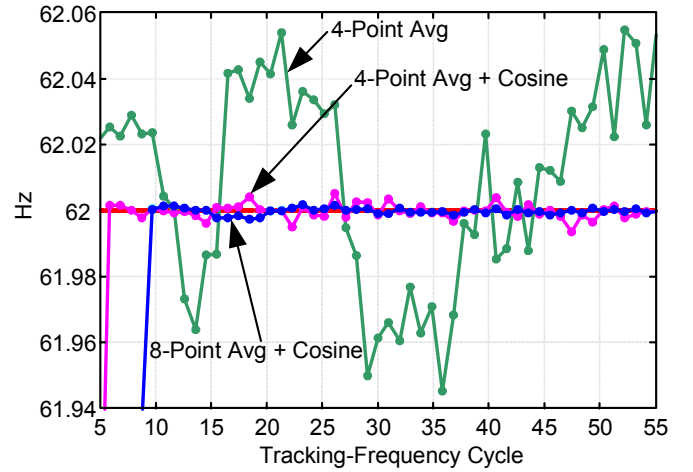


Fig. 7. Frequency Measurement With a Noisy Input

B. Frequency Tracking

With an accurate power system frequency measurement, the relay can adjust the sampling frequency so that it always maintains an integer number of samples per cycle regardless of the system frequency. In the following, we use the terms frequency tracking and sampling frequency interchangeably. There are several considerations when adapting the sampling frequency to the system frequency. Choices for these parameters decide tracking algorithm performance:

- Upper frequency tracking limit
- Speed of frequency tracking
- Dead band of frequency tracking

Protective relay elements are executed in real time. Microprocessor relays typically use an interrupt-driven mechanism to guarantee protective element calculation and updating in a given time. With a 60 Hz nominal system and a relay that samples at 16 samples per cycle, an interruption routine occurs every 16th of one 60 Hz cycle, or about every 1.04 ms. Within this time frame, the relay must finish all required protective element calculations. The relay must also leave some time for increasingly demanding background communications, automation, and man-machine interfaces. If the input frequency increases to 70 Hz, the relay must finish the same amount of calculations within 0.89 ms. If the relay already has 100 percent burden at the nominal frequency, requiring the relay to track the frequency to 70 Hz will necessitate replacement of the microprocessor with one that has 16.7 percent additional processing power. It is therefore impractical for a microprocessor relay to track to an arbitrarily high frequency. An upper frequency-tracking limit is in place to ensure that the relay can finish required tasks at that upper frequency limit. An alternative is to use the frequency difference to compensate a phasor for off-nominal frequency errors. Relay sampling frequency can then be fixed at the nominal frequency.

It is possible to adapt the sampling frequency to the instantaneously measured system frequency. This accelerates the frequency tracking process, but the relay can also track to erroneous frequency quickly and cause phasor calculation errors. To stabilize the frequency tracking process, a relay can correct a percentage of the difference between the measured

and the sampling frequency. One choice for this correction is an Infinite-Impulse Response (IIR) filter type of frequency update:

$$f_{s,k} = \alpha(f_{m,k} - f_{s,k-1}) + f_{s,k-1} = \alpha f_{m,k} + (1-\alpha)f_{s,k-1} \quad (12)$$

where f_s is sampling frequency and f_m is frequency measurement. The variable k is the present processing interval and $k - 1$ is the previous processing interval. The variable α is a constant that, with a sampling frequency updating rate of PR, relates to the time constant TC by (13).

$$\alpha = 1 - e^{-\frac{1}{PR \cdot TC}} \quad (13)$$

For example, if a relay updates sampling frequency every other zero-crossing detection (one cycle), and α is 1/8, the time constant is about 7.5 cycles. In 7.5 cycles, the relay corrects 63 percent of any difference between sampling frequency and measured frequency.

To prevent the frequency-tracking algorithm from hunting small frequency measurement errors, a relay can implement a dead band such that when the frequency difference falls inside this band, the tracking algorithm stops following the input frequency. This dead band is normally quite small and has no significant impact on frequency tracking performance.

Fig. 8 shows the frequency tracking to a 2-Hz step change. The frequency-tracking α constant is 1/8 in (12), but the sampling frequency updates every two input-frequency cycles. We can readily check the time constant of 15 cycles from the figure.

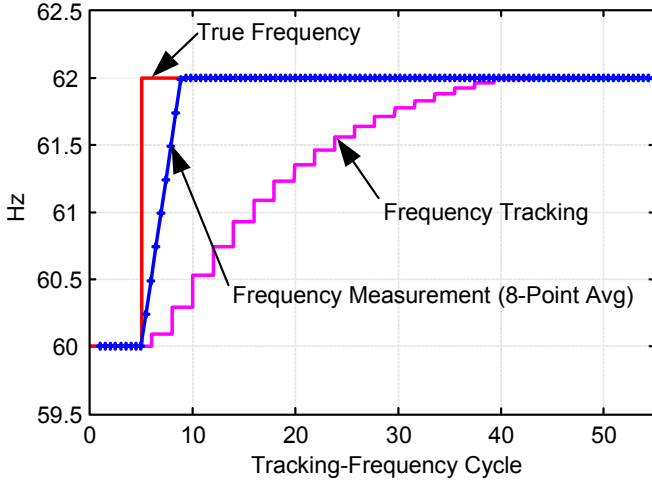


Fig. 8. Frequency Measurement and Tracking to a 2-Hz Step Change

Because of the time delay in the frequency measurement and the frequency tracking, the initial mismatch between the sampling and input frequencies results in a phasor calculation error, as Fig. 9 shows. Note that, as we discussed previously, the A-phase voltage has a magnitude oscillation twice the input frequency. However, this same oscillation is absent in the positive- and negative-sequence quantities because of the smoothing effect of three phases [2]. We also observe that the phasor errors of three phases cancel out in the zero-sequence quantity so that the zero-sequence voltage remains zero even if the sampling frequency does not match the input frequency.

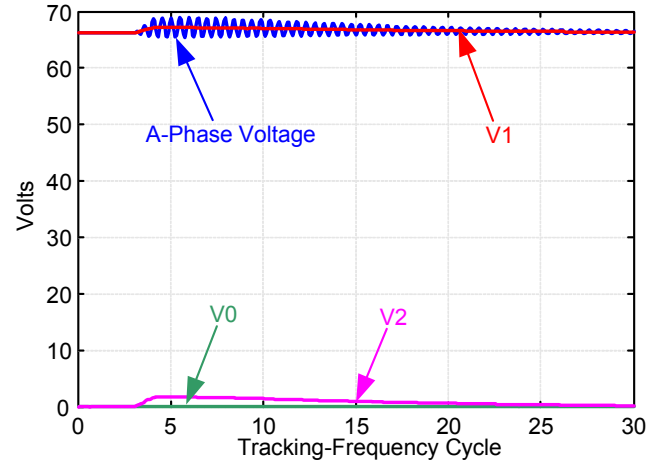


Fig. 9. Voltages During Frequency Tracking to a 2-Hz Step Change

Fig. 10 shows the frequency tracking to a 5 Hz per second ramp frequency change. This type of ramp change is close to what we could see in a real situation of sudden load or generation rejection.

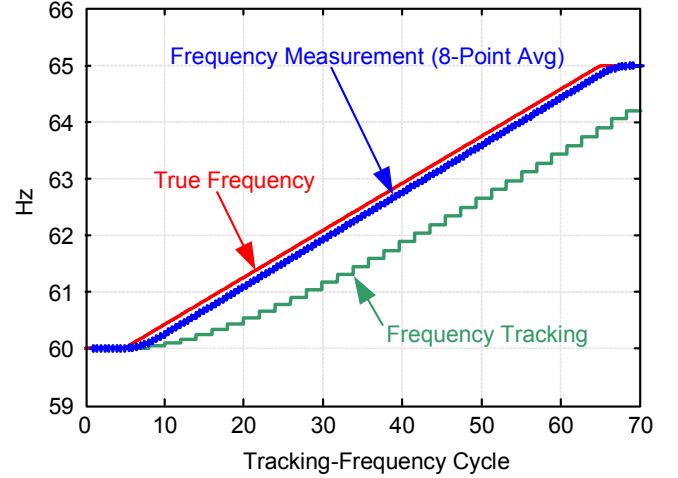


Fig. 10. Frequency Measurement and Tracking to a 5 Hz/sec Ramp Change

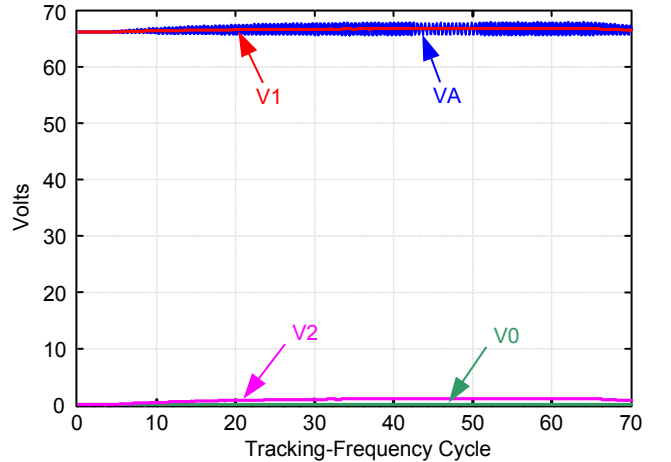


Fig. 11. Voltages During Frequency Tracking to a 5 Hz/sec Ramp

With the same time constant of 15 cycles, we observe that there is a constant difference of about 1 Hz between the measured and sampling frequencies. This constant mismatch results

in a constant phasor calculation error as Fig. 11 shows. By changing the α constant to 1/2, we reduce the time constant to less than three cycles.

Fig. 12 and Fig. 13 show the frequency tracking and voltage magnitudes with this reduced time constant. We see that the sampling frequency is much closer to the input frequency and that the phasor calculation error, therefore, is proportionally smaller.

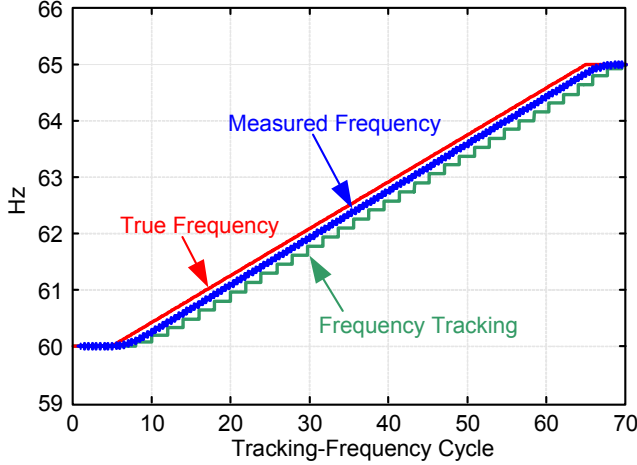


Fig. 12. Frequency Tracking to a 5 Hz/sec Ramp Change With a Smaller Time Constant

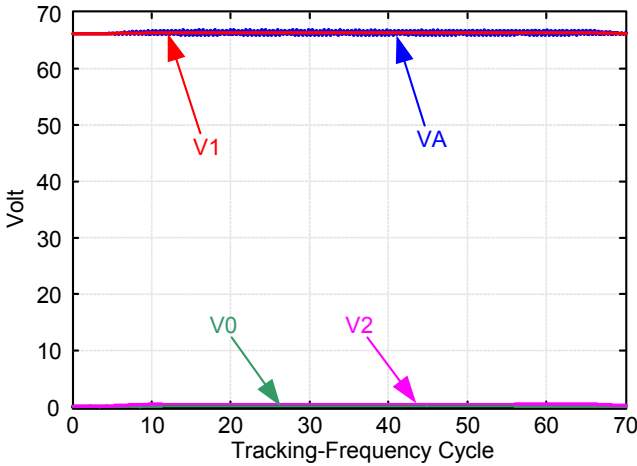


Fig. 13. Voltages During Frequency Tracking to a 5 Hz/sec Ramp With a Smaller Time Constant

1) Frequency Lag During an Input Frequency Ramp Change

At the onset of an input frequency ramp change, the initial frequency difference, $f_{m,k} - f_{s,k-1}$, is small, and the sampling frequency updates slowly per (12). When this frequency difference gets larger, each frequency update step becomes larger, and the sampling frequency eventually matches the rate of change of the input frequency. We can observe this in Fig. 10.

This IIR sampling frequency update process leaves behind a frequency difference between the sampling and input frequencies. Use (12) to evaluate the magnitude of this frequency difference. Rearrange (12) to obtain (14):

$$\begin{aligned} f_{s,k} - f_{s,k-1} &= \alpha(f_{m,k} - f_{m,k-1}) - \alpha f_{s,k-1} + \alpha f_{m,k-1} \\ &= \alpha(f_{m,k} - f_{m,k-1}) - \alpha(f_{s,k-1} - \alpha f_{m,k-1}) \end{aligned} \quad (14)$$

When the sampling frequency matches the rate of change of the input frequency, we have $f_{s,k} - f_{s,k-1} = f_{m,k} - f_{m,k-1}$, and (14) becomes the following:

$$f_{m,k} - f_{m,k-1} = \alpha(f_{m,k} - f_{m,k-1}) - \alpha(f_{s,k-1} - \alpha f_{m,k-1}) \quad (15)$$

We then find the frequency difference as follows:

$$f_{s,k-1} - f_{m,k-1} = \frac{\alpha-1}{\alpha}(f_{m,k} - f_{m,k-1}) = \frac{\alpha-1}{\alpha}\Delta f_m \quad (16)$$

Equation (16) tells us that the frequency difference is constant and proportional to the rate of change of measured frequency. The update factor α directly impacts this frequency difference. Note that Δf_m in (16) must be in Hz per every updating period k . With a 5 Hz/sec. ramp change and the same sampling frequency update rate of every two input-frequency cycles, we have $\Delta f_m = 2 \cdot 5 / (\text{measured frequency cycles per second})$. Using the nominal 60 cycles per second as an approximation, we have $\Delta f_m = 1/6$ Hz per every two input cycles. Table I lists the constant frequency difference for several input frequency ramp rates with $\alpha = 1/8$.

TABLE I
DIFFERENCE BETWEEN SAMPLING AND INPUT FREQUENCIES FOR DIFFERENT INPUT FREQUENCY RAMP RATES

$\Delta f/\text{sec.}$	Δf
5 Hz/sec.	-1.17 Hz
10 Hz/sec.	-2.33 Hz
15 Hz/sec.	-3.50 Hz
20 Hz/sec.	-4.67 Hz

IV. PROTECTION ELEMENTS AND PERFORMANCE UNDER FREQUENCY EXCURSIONS

Phasor errors from the difference between a relay sampling frequency and the input frequency directly affect the performance of relay protective elements. Although most microprocessor relays use an adaptive sampling frequency to keep the number of samples per input signal cycle constant, we have seen from previous sections that the sampling frequency lags the input frequency more or less according to the design of frequency measurement and tracking algorithms.

Depending on the operating principle of each protection element, it behaves differently under the same frequency excursion condition. In this section, we evaluate the performances of three representative protection elements, magnitude protection, differential protection, and impedance protection.

A. Magnitude Protection Element

Magnitude protection elements calculate the magnitude of a phasor and compare it with a set threshold to make a protection decision. These elements include the following:

- Overcurrent or overvoltage: $|V| > V_{th}$
- Undervoltage or undercurrent: $|V| < V_{th}$
- Voltage or current conditions: $V_{th1} < |V| < V_{th2}$, or $|V| < V_{th1}$ and $|V| > V_{th2}$

In most applications, the magnitude protection elements have a time delay to coordinate with other protection devices. The time delay can have a definite-time or an inverse-time characteristic.

We have seen the impact to phasor magnitudes when there is a frequency excursion. The phasor magnitude oscillates at twice the input signal frequency. The oscillation magnitude is proportional to the frequency difference between the sampling and input frequencies. Development of the exact relationship between the oscillation magnitude and the frequency difference is mathematically involved and is very sensitive to the the phasor derivation process. For example, adding a simple differentiator to the one-cycle Fourier filter dramatically changes the frequency excursion impact to the phasor magnitude, as Fig. 14 shows.

Fig. 14 shows the magnitude oscillations of a phasor from a Fourier filter plus differentiator as a function of the frequency difference between the input and sampling frequencies. From the figure, we see that the oscillation has a complete positive offset for input frequencies greater than the sampling frequency, and a complete negative offset for input frequencies less than the sampling frequency. Input frequencies greater than the sampling frequency impact overcurrent and overvoltage elements, while input frequencies less than the sampling frequency impact undercurrent and undervoltage elements.

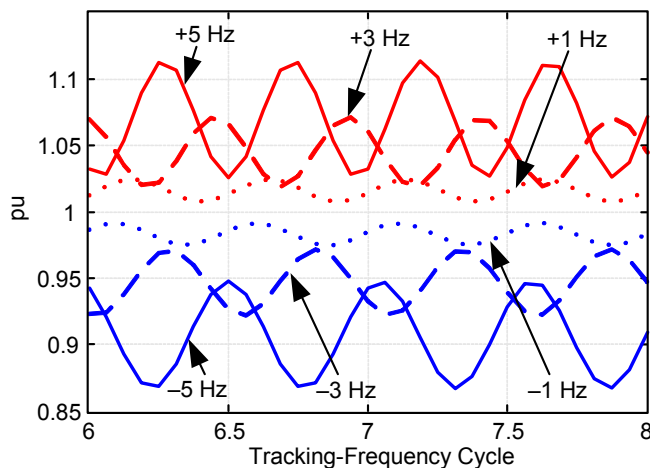


Fig. 14. Magnitude Oscillation of a Phasor From Fourier Filter Plus Differentiator

Fig. 15 shows similar magnitude oscillations of a phasor from a cosine filter and quarter-cycle delay. One difference from the Fourier filter in Fig. 14 is that for input frequencies much greater than the sampling frequency, the cosine filter causes the phasor magnitude to be less than the true value. For example, when the input frequency is 5 Hz greater than the sampling frequency, the phasor magnitude can be as high as 9.1 percent above the true magnitude at the peaks of oscillation, and as low as 4 percent below the true magnitude. It therefore impacts both over- and undermagnitude protection elements. Observe that the input frequency 5 Hz less than the sampling frequency only causes about one percent error greater than true magnitude. The oscillations that high- and low-input frequencies cause are not symmetrically centered about the true magnitude.

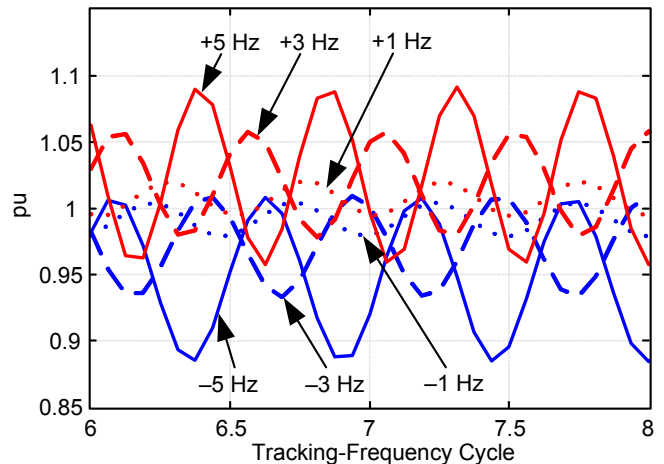


Fig. 15. Magnitude Oscillation of a Phasor From Cosine Filter

Disregarding the minor magnitude error on the opposite side, Table II summarizes the maximum phasor magnitude error for different input frequencies above and below the sampling frequency for cosine plus a quarter-cycle delay and Fourier plus differentiator filters. Remember that these errors result from previous assumptions for frequency measurement and tracking.

TABLE II
PERCENTAGE MAGNITUDE ERROR FOR FREQUENCY DIFFERENCES BETWEEN THE INPUT AND SAMPLING FREQUENCIES

Δf	Cosine	Fourier + DT
-5 Hz	-11.6	-13.3
-3 Hz	-6.7	-7.8
-1 Hz	-2.2	-2.5
+1 Hz	2.1	2.5
+3 Hz	5.8	7.2
+5 Hz	9.1	11.4

For critical protection applications, one should evaluate the power system and set the protection threshold accordingly. For example, if the system frequency could ramp up at 10 Hz per second after a load rejection, Table I indicates that the input frequency may eventually be 2.33 Hz greater than the sampling frequency. From Table II, this frequency difference causes about +7 percent magnitude error. One should increase the overcurrent or overvoltage setting thresholds accordingly to prevent possible misoperation. Definite time delays reduce or eliminate the impact of such magnitude errors. The inverse-time elements tend to smooth out the peaks and valleys of the magnitude oscillation and provide an output based on the average of the input.

1) A Real-World Example

In a load rejection test with a 13.2 kV hydroelectric generator, a 60 MW and 43 Mvar load was rejected. The generator sped up and generator frequency increased exponentially, as Fig. 16 shows.

A phase overvoltage element is set at 14.9 kV with a 0.5-second delay. After the load rejection, we see that the generator terminal voltage increased slowly from 13.6 kV to 14.4 kV. However, this increase was insufficient to cause phase overvoltage element operation. The relay has an upper frequency-tracking limit of 70 Hz.

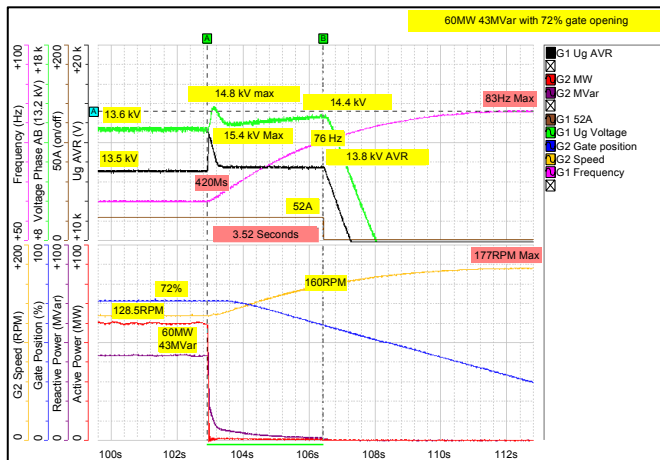


Fig. 16. A Hydroelectric Generator Frequency Change After a 60 MW Load Rejection

Fig. 17 shows the phase-to-phase voltage measurement from the relay. The relay voltage magnitudes are generally in line with the input frequency. This frequency is 5 Hz higher than the sampling frequency, causing oscillation peaks 9 percent (or 15.48 kV in this case) greater than the true magnitude. Note that this phase overvoltage element operates on the maximum phase-to-phase voltage. Fig. 17 indicates that the maximum phase-to-phase voltage is always greater than 15 kV, causing the 0.5-second delay-pickup timer to time out.

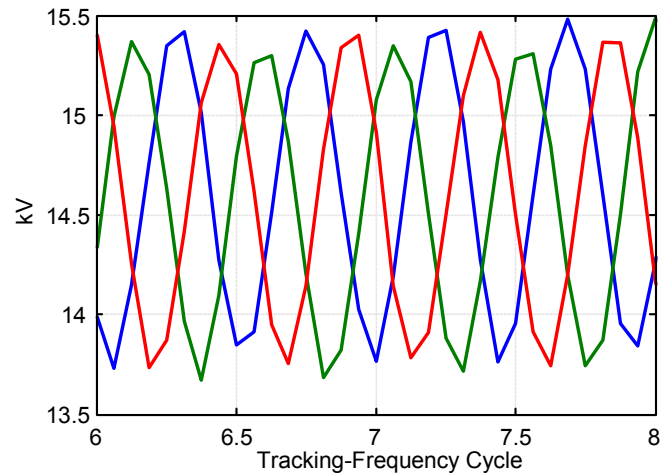


Fig. 17. Phase-to-Phase Voltage Measurement From the Relay

B. Differential Protection Element

Current differential protection is popular for transmission line, transformer, reactors, and motor protection. It operates on a simple principle that the current going into an apparatus must equal the current leaving the device when there is no fault.

Fig. 18 shows a current differential protection scheme for a two-terminal device. A relay measures currents at both ends of the apparatus. A phasor sum of all currents provides an operating current (IOP) for the current differential protection. There are different ways to set up the restraining current for the differential element [3]. Equation (17) shows the most popular restraining current (IRT), which is an average of two current magnitudes for two-terminal devices.

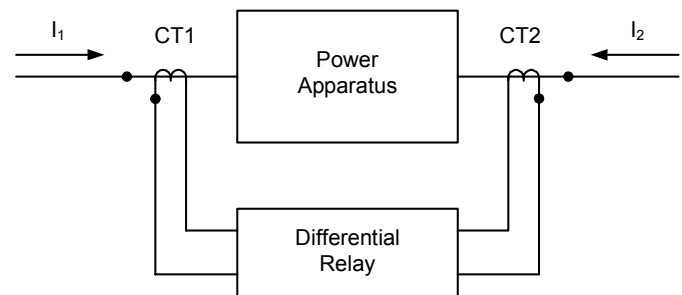


Fig. 18. Current Differential Protection Scheme

$$IOP = |I_1 + I_2|; \quad IRT = \frac{|I_1| + |I_2|}{2} \quad (17)$$

Fig. 19 shows the operating characteristic of the percentage-restrained current differential protection. A settable percentage of the restraining current determines the restraining quantity for this differential element. Fig. 19 shows this percentage as Slope1. The relay compares the operating current to the restraining quantity. The percentage current differential element operates when the operating current is greater than both the restraining quantity and a minimum pickup threshold.

The differential element typically provides a second slope. This second slope, which Fig. 19 shows as Slope2, is greater than the first slope. When fault currents exceed a certain level as determined by IRS1, the operating current must overcome a

greater percentage of the restraining current as determined by Slope2. Slope 2 provides secure element operation under conditions, such as CT saturation, where large fault currents could result in large measurement errors.

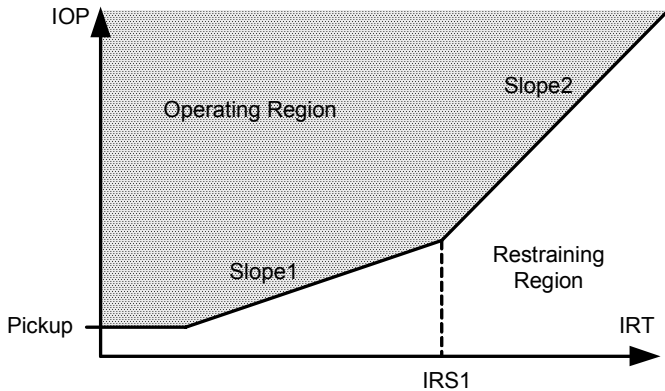


Fig. 19. Differential Element Operating Characteristic

Now let's examine the differential element operations when there is a system frequency excursion and the input current frequency does not match the relay sampling frequency. For the following, we assume that the frequency of input currents is 5 Hz greater than the sampling frequency. Fig. 20 shows the operating and restraining currents that the relay measures for an external fault. For external faults, if we disregard the small (line) charging current that leaks out inside the device under protection, the current I_2 in Fig. 18 equals the negative I_1 , or $I_2 = -I_1$. Both currents are the same phasor with opposite polarity. When the relay calculates a phasor sum, the phase shifts and magnitude oscillations in two phasors cancel out. Fig. 20 shows that the resulting operating current is a perfect zero. We observe that a system frequency excursion does not affect the security of the differential element for external faults.

Because the restraining current is an average of phasor magnitudes, the magnitude oscillations of an individual phasor pass directly to the restraining current, as Fig. 20 shows.

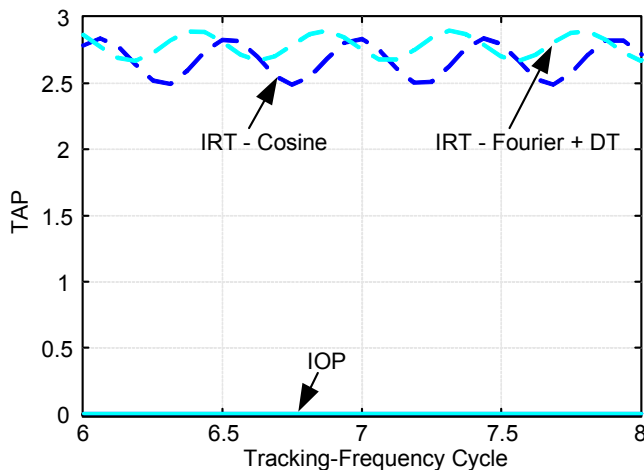


Fig. 20. Operating and Restraining Currents for an External Fault

For a zero-fault-resistance internal fault, Fig. 21 shows the operating and restraining currents that the relay measures. In

this case, both operating and restraining currents oscillate with a similar percentage magnitude error, as we can see from Table II.

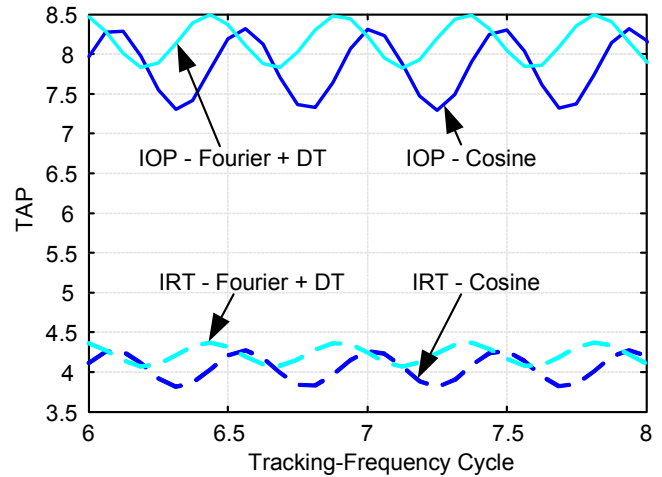


Fig. 21. Operating and Restraining Currents for an Internal Fault

Plotting the operating current against the restraining current, we obtain the element trajectory on the operating characteristic plane in Fig. 22. The figure shows both element loci of the external fault of Fig. 20 and the internal fault of Fig. 21. The dots labeled "Internal Fault" and "External Fault" are the static points for these faults when the system frequency matches the relay sampling frequency.

From Fig. 22, we see that the differential element is secure again for external faults, regardless of system frequency excursions. The figure also shows dependable operation of the element for this internal fault without fault resistance. The operating current oscillations resulting from system frequency excursions can reduce the sensitivity of the element to high-resistance faults. However, this impact to sensitivity is minimal; the strong through current for high-resistance faults tends to cancel out the oscillation.

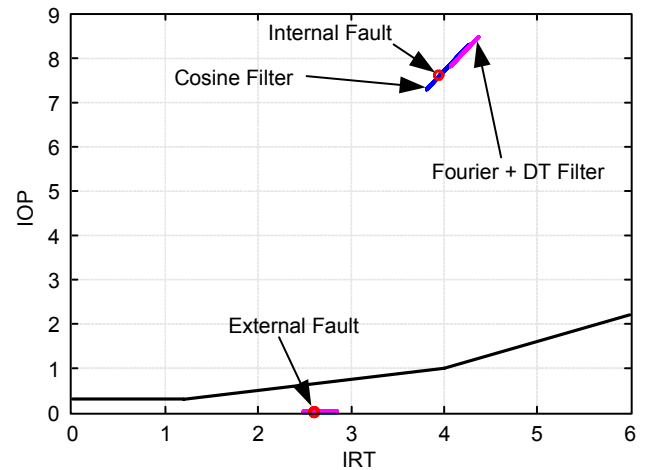


Fig. 22. Impact of 5 Hz Frequency Difference Between Sampling and Input

C. Impedance (Distance) Protection Element

The impedance protection element measures apparent impedance from a substation to a fault, compares this impedance

with the line impedance, and decides if the fault is inside a protection zone. To expand the protection element to cover more fault arcing resistance, we often use phase comparators to form a mho impedance element that has a circular operating characteristic [4]. We also often use a quadrilateral operating characteristic for ground distance elements to allow even larger fault resistance. The impedance protection element is the most challenging element to design and understand, because there exist many choices for operating characteristic shape, polarizing quantities, and associated dynamic/expanding characteristic.

Fig. 23 shows a mho characteristic of an impedance element. The element tests the angle difference of an operating quantity dV and a polarizing quantity V_{POL} . The element operates if the operating quantity is within 90° of the polarizing quantity, otherwise it restrains. Therefore, the operating region in Fig 23 is inside the mho circle. When a fault occurs at the limits of the reach setting, this angle is 90° .

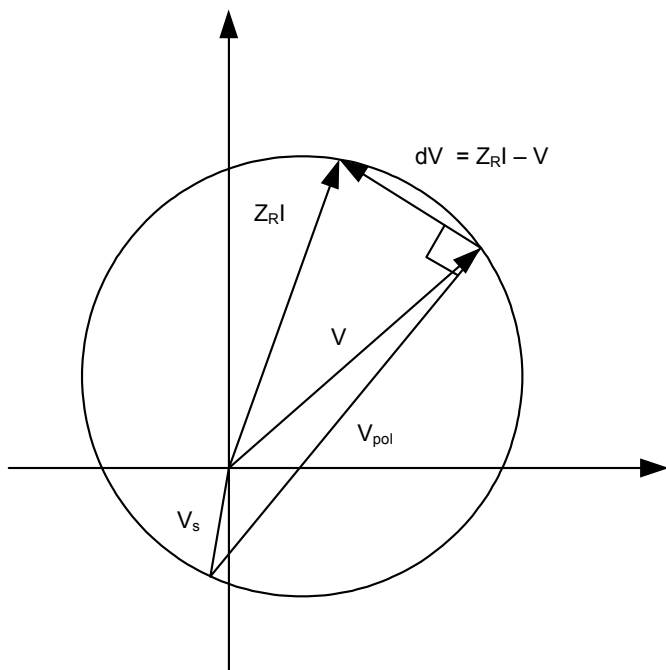


Fig. 23. Development of Mho Characteristic

The following equation implements the mho element. The asterisk in the equation represents the complex conjugate. When the result P is greater than or equal to zero, the element operates. The element restrains if the result P is negative.

$$P = \text{real}(dV \cdot V_{POL}^*) \quad (18)$$

Positive-sequence voltage is a popular polarizing quantity for modern microprocessor relays. It is equivalent to cross polarizing that uses a combination of unfaulted phase voltages and therefore operates for a zero-volt unbalanced fault. It also expands the operating characteristic, similarly to cross polarizing, back to the system source, as Fig. 23 shows. For close-in three-phase faults, relays memorize the pre-fault voltage reference and allow the element to operate reliably for a loss of all voltages.

Reference [4] mapped all points on a mho circle into a simple number, m . The relay then tests this m against different reach settings and obtains multiple zones of protection with a single calculation. For boundary faults on the mho circle, we can obtain the following from (18):

$$0 = \text{real}(dV \cdot V_{POL}^*) = \text{real}[(Z_R I - V) \cdot V_{POL}^*] \quad (19)$$

Then, the reach for this fault in terms of percentage of the line impedance Z_L is ($Z_R = mZ_L$):

$$m = \frac{\text{real}(V \cdot V_{POL}^*)}{\text{real}(Z_L I \cdot V_{POL}^*)} \quad (20)$$

We use a simple two-source system such as Fig. 24 illustrates to demonstrate what occurs to the impedance element when the relay-tracked frequency is different from that of the inputs.

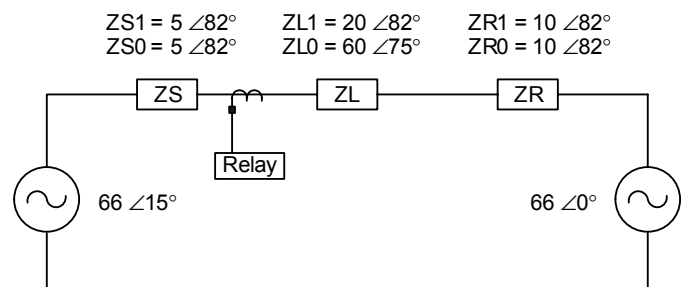


Fig. 24. A Simple Two-Source System to Evaluate Off-Frequency Performance of Impedance Element

Fig. 25 shows the m calculation using cosine filtering for an A-phase-to-ground fault at the end of the line in Fig. 24. For the simulation, the element uses the positive-sequence voltage as the polarizing quantity. The simulation assumes a 5 Hz difference between the relay-tracking and input frequency. Without the frequency difference, the m value should be 1.0. However, we see that the frequency difference causes variations in the m value similar to the variations in the phasor magnitude. The oscillation of the impedance calculation is more symmetrical around the true value than that of the phasor magnitude. The percentage of impedance variation is very close to those in Table III, about 12 percent for this 5 Hz frequency difference.

Fig. 25 shows an A-phase fault occurring simultaneously with a system frequency excursion. The relay would have overreached by 12 percent in this case. In general, a relay measures the load impedance when system frequency excursion occurs. As long as the system is not heavily loaded, the error of impedance calculation that a frequency difference causes would not encroach upon the mho-operating characteristic.

When an impedance element uses a memory with the polarizing quantity, a frequency excursion causes an impedance calculation error in addition to the error we discussed previously.

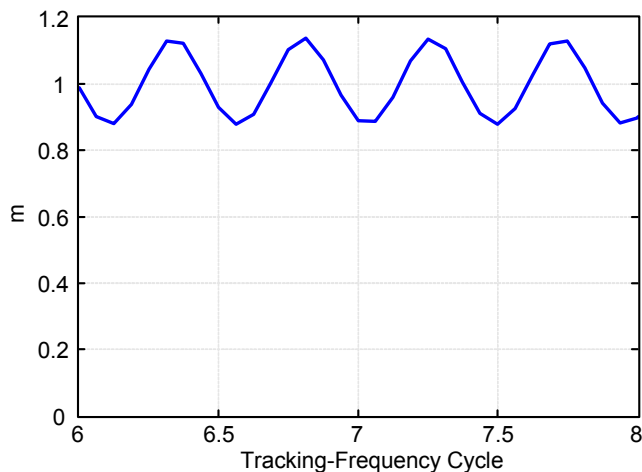


Fig. 25 M Calculation for AG Fault at the End of Line With a 5 Hz Frequency Difference

Fig. 26 from [5] shows the polarizing problem during a minus 9 Hz-per-second frequency excursion after cycle 5. There is no fault on the monitored line. The initial m calculation of 260 before cycle 5 is a result of system load flow. Approximately 30 cycles after the initial frequency excursion occurs, the impedance calculation goes below 0.85, the normal zone 1 distance reach setting. The relay would therefore inadvertently trip because of the frequency excursion and the use of a long polarizing memory.

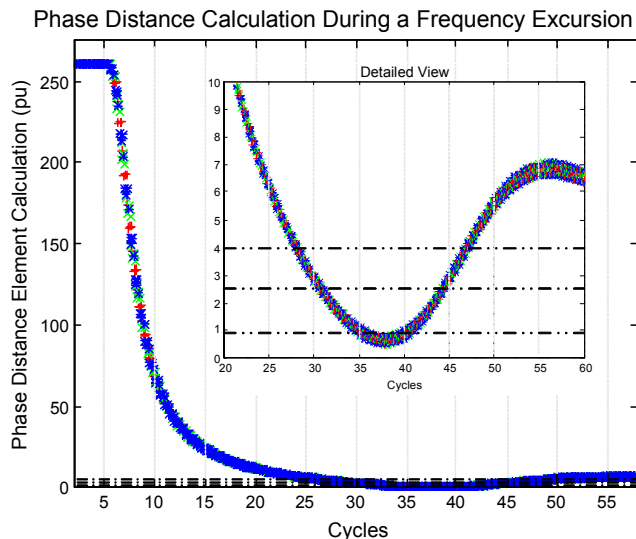


Fig. 26. M Calculation of Phase Mhos During a Frequency Excursion

Fig 27 illustrates why a memory polarized impedance element might operate during a frequency excursion. Fig 27(a) shows the phasor relationship between the operating quantity, $Z_{R1} - V$, and the polarizing quantity, V_{POL_MEM} , during a normal load condition. We see that the operating and polarizing quantities are close to 180° for a light load condition. When a frequency excursion occurs, the relay tracks to the new frequency. Because of the memory effect, the angle of the polarizing quantity starts to slip away from the input voltage. If this frequency excursion persists, the angle difference between

$Z_{R1} - V$ and V_{POL_MEM} becomes less than 90° , as Fig. 27(b) shows, and the mho element operates.

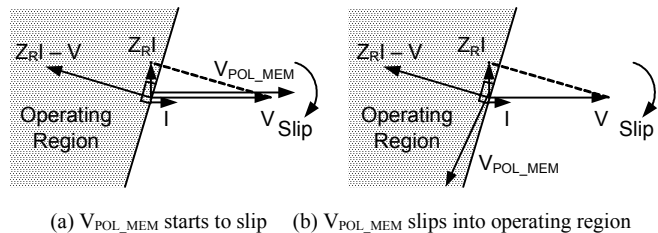


Fig. 27. A Frequency Excursion Causes the Memorized Polarizing Quantity to Rotate Into Operating Region

From the type of memory that the polarizing quantity uses, we can determine the approximate length of frequency excursions that the impedance element can withstand without misoperating. One popular type of memory uses a first-order IIR filter to obtain the memory effect:

$$V_{POL_MEM,k} = \alpha V_{I,k} + (1 - \alpha)V_{POL_MEM,k-1} \quad (21)$$

Similarly, (13) relates α to the memory time constant TC . To estimate the length of a frequency excursion that an impedance element can take without misoperating, let's make the following assumptions:

- $V_{I,k}$ advances by ϕ degrees in one memory updating processing interval (k) in a frequency excursion.
- $V_{POL_MEM,k-1}$ starts at the zero-degree reference angle.
- $V_{I,k}$ and $V_{POL_MEM,k-1}$ have the same magnitude $|V|$.

Then the new polarizing voltage is as follows:

$$\begin{aligned} V_{POL_MEM,k} &= |V| [\alpha e^{j\phi} + (1 - \alpha)] \\ &= |V| [\alpha(\cos \phi - 1) + j \sin \phi] \end{aligned} \quad (22)$$

The angle advance for the new polarizing voltage is as follows:

$$\angle V_{POL_MEM,k} = \tan^{-1} \frac{\sin \phi}{\alpha(\cos \phi - 1) + 1} \quad (23)$$

In one processing interval, the angle of the new memory polarizing quantity lags that of the input by the following:

$$\Delta \phi = \phi - \tan^{-1} \frac{\sin \phi}{\alpha(\cos \phi - 1) + 1} \quad (24)$$

The time that the impedance element misoperates is the time during which the number processing intervals accumulate $\Delta \phi$ to 90° . For example, if a frequency excursion causes a 5 Hz difference between the tracking and input frequencies, and if the memory voltage updates every half cycle, ϕ equals 15° based on 60 Hz cycles. If the memory updating constant α is 0.25, then $\Delta \phi$ equals to 0.37° for each processing interval. It then takes about 240 processing intervals for the angle difference to accumulate to 90° , or roughly two seconds for the impedance element to misoperate.

V. CONCLUSION

A mismatch between the relay sampling frequency and input frequency causes phase and magnitude oscillating errors in phasor calculation. The amount of error is proportional to the frequency difference and depends also on the type of filters in use for phasor extraction.

When a relay employs a frequency tracking scheme to adapt sampling frequency to that of the input frequency, the relay cannot track to an arbitrarily high frequency because of limited processing power. The relay also introduces delays in the frequency measurement to ensure accuracy and delays in tracking to stabilize the sampling frequency. When the system frequency slew rate is constant, the frequency measuring and tracking delay introduce a fixed steady-state frequency difference. The slower the frequency tracking, the larger the frequency difference.

Different protection elements behave differently during a system frequency excursion. The accuracy of magnitude protection elements such as overcurrent elements relates directly to the magnitude oscillation of a phasor during a frequency excursion. The amount of overcurrent overreach is proportional to the difference between the input and relay tracking frequencies. This difference depends on the input frequency slew rate and the speed of the frequency tracking algorithm.

For the current differential element, the calculation of the operating quantity cancels out the phase and magnitude errors of phasors for external faults. The element therefore remains secure for external faults regardless of input frequency changes. For internal faults, the operating quantity has the usual oscillations similar to those of phasor magnitudes during a frequency excursion. The element should be dependable for an internal fault except in those extreme boundary cases when fault resistance is large.

The performance of the distance element relates closely to how the relay uses memory for the polarizing quantity. With positive-sequence or cross polarization, the element incurs oscillating errors similar to that of the phasor magnitude. This type of error is generally not a concern for lightly loaded systems. When a memory is used for the polarizing quantity, a system frequency excursion can eventually cause the distance element to misoperate for a persistent excursion. For a polarizing memory that uses an IIR type of filtering, the frequency excursion duration that a distance element can handle without misoperation depends on the IIR filter time constant.

VI. REFERENCES

- [1] E. O. Schweitzer, III and D. Hou, "Filtering for Protective Relays," in *1992 19th Annual Western Protective Relay Conference Proceedings*.
- [2] *Advancements in Microprocessor Based Protection and Communication*, IEEE Tutorial Course, Piscataway, NJ: The Institute of Electrical and Electronics Engineers, 1997.
- [3] A. Guzman, S. Zocholl, G. Benmouyal and H. J. Altuve, "A Current-Based Solution for Transformer Differential Protection--Part 1: Problem Statement," *IEEE Trans. Power Delivery*, vol. 16, no. 4, Oct. 2001.
- [4] E. O. Schweitzer and J. Roberts, "Distance Relay Element Design," in *1992 19th Annual Western Protective Relay Conference Proceedings*.
- [5] D. Hou, A. Guzman and J. B. Roberts, "Innovative Solutions Improve Transmission Line Protection," in *1997 24th Annual Western Protective Relay Conference Proceedings*.

VII. BIOGRAPHIES

Daqing Hou received B.S. and M.S. degrees in Electrical Engineering at the Northeast University, China, in 1981 and 1984, respectively. He received his Ph.D. in Electrical and Computer Engineering at Washington State University in 1991. Since 1990, he has been with Schweitzer Engineering Laboratories, Inc., Pullman, Washington, USA, where he has held numerous positions including development engineer, application engineer, and R&D manager. He is currently a principal research engineer. His work includes system modeling, simulation, and signal processing for power systems and digital protective relays. His research interests include multivariable linear systems, system identification, and signal processing. He holds multiple patents and has authored or co-authored many technical papers. He is a Senior Member of IEEE.